CMOS-Compatible Wideband Silicon Modulator

S. J. Spector[1*], M. W. Geis[1], G.-R.Zhou[2], M. E. Grein[1], R. T. Schulein[1], F. Gan[2], M. A. Popović[2], J. U. Yoon[1], D. M. Lennon[1], E. P. Ippen[2], F. X. Kärtner[2], and T. M. Lyszczarz[1]

[1]*Lincoln Laboratory, Massachusetts Institute of Technology, Lexington, MA 02420, USA*

[2]*Research Laboratory of Electronics, Massachusetts Institute of Technology, Cambridge, MA 02139, USA*

**spector@LL.MIT.EDU*

Abstract: A Mach-Zehnder based silicon optical modulator has been demonstrated with a bandwidth of 26 GHz and a VπL of 2 V·cm. The design of this modulator does not require an epitaxial overgrowth.

1. Introduction

The development of silicon based photonics has the potential to allow monolithically-integrated, low-cost optical devices on a platform compatible with CMOS circuits. Optical modulators are an essential component in most applications, and there has been a large amount of recent effort in developing silicon based optical modulators. The fastest silicon modulator, to date, used carrier depletion in a p-n diode [1]. One disadvantage to the design in [1] is the use of a top contact which requires an epitaxial silicon overgrowth. The design described here does not use a top contact, and therefore eliminates that expensive fabrication step with no apparent loss in performance. The modulator demonstrated here achieves 26 GHz of bandwidth and a VπL of 2 V·cm.

2. Design

The modulators are fabricated using Unibond silicon-on-insulator (SOI) wafers with a 0.22 μm thick layer of silicon above a 3 μm buried oxide. Fig. 1(a) schematically shows the top-view of the modulator. The active areas of the device are p-n diode phase shifter sections in the arms of the modulator. By employing a relatively short interaction length of 0.5 mm, (the travel time of the light is only 5 ps), a simple lumped element electrode can be used to achieve speeds of about 30 GHz. The modulator can be operated in a push-pull configuration by driving the center electrode (as shown), or a single arm can be driven. An additional thermal phase shifter (not shown) is fabricated on one arm, to allow the modulator to be driven at quadrature, regardless of the bias on the diodes.

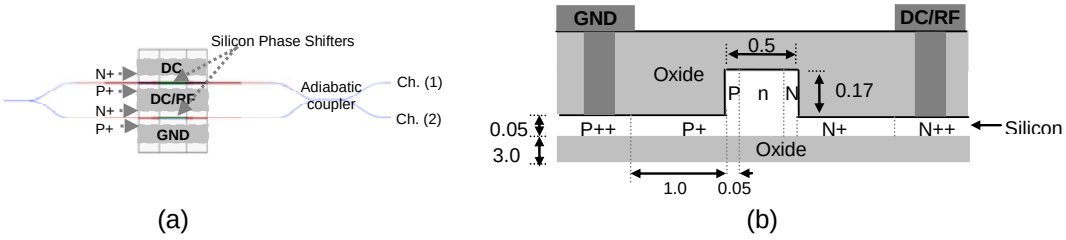

Figure 1. (a) Top-view layout of the dual-output modulator. (b) Schematic view of the cross-section of one of the phase shifters. (All dimensions are in μm).

An adiabatic output-coupler [2] is used to combine the two arms of the Mach-Zehnder interferometer, instead of the more standard y-coupler. This type of output-coupler provides low loss, broadband functionality, and two complementary outputs (channels 1 and 2) from the modulator. The two complementary outputs can be used in analog applications to linearize the transfer function of the modulator and compensate for fluctuations external to the modulator [3,4]. To provide efficient coupling on and off the wafer, reverse taper couplers combined with lower index oxynitride waveguides [5] are used.

Fig. 1(b) shows schematically the cross-section of the waveguide in the active area of the modulator. The central region, or core of the waveguide is 220 nm thick, 500 nm wide, and lightly n-type doped to a concentration of 2×10^{17}cm^{-3}, resulting in a break down voltage of 16 V. The sidewalls are moderately doped, n-type on one side and p-type on the other, to a concentration of 10^{18} cm^{-3} and an approximate depth of 50 nm. When a reverse bias is applied, a depletion region forms at the p-n junction on one side of the waveguide. This depletion region's size increases into the center of the waveguide as the bias is increased, creating a change in the refractive index of the waveguide. To make electrical contact to the core of the waveguide, heavily doped, (10^{19} cm^{-3} concentration), 50

nm thick slab regions connect the waveguide to metal contacts located 1 μm away. To ensure good ohmic contact, the silicon slab under the metal contacts is degenerately doped to a concentration of 10^{21} cm^{-3}. The parasitic resistance of the diodes including ohmic contacts and the resistance of the doped Si is usually <0.3 Ω cm.

3. Results

To model the carrier concentration in the waveguide, numerical simulations were performed by solving Poisson and carrier continuity equations. The modeled change in carrier concentration determines a change in the material index of silicon which can then be used to determine the change in the modal index, N_{eff}. The simulations show that the application of a reverse bias of 8 V causes an increase in the modal index, ΔN_{eff}, of ~1.67×10^{-4} as well as an increase in the absorption coefficient, $\Delta\alpha$, of ~$1.61 cm^{-1}$. With an interaction length of 0.5 mm, this corresponds to a phase change $\Delta\phi$ of 0.11π and absorption loss of 0.34 dB.

The DC response of the modulator was tested by varying the DC bias voltage on arm #1 while the other arm remained at the same bias level. Fig. 2 shows the simulated and measured normalized light intensity as a function of the applied voltage, for the two complementary outputs. The measured and simulated results are in good agreement with each other. To get a better measure of $V\pi L$, a longer device, with 5 mm arm lengths, was also measured. The output of that modulator is also shown in Fig. 2, and gives a $V\pi L$ of just over 4 V·cm. This is comparable to what had been achieved earlier with a more complicated structure [1]. Operating the modulator in a push-pull configuration cuts $V\pi L$ in half to 2 V·cm, as expected.

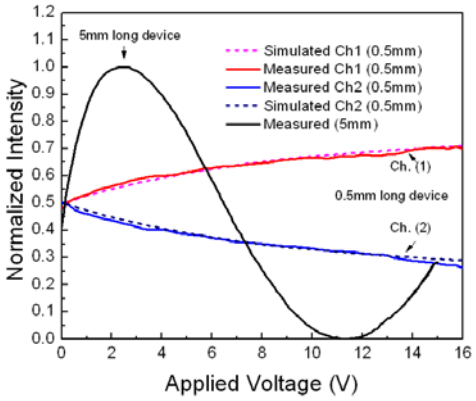

Figure 2. Measured and simulated normalized light transmission as a function of applied voltage.

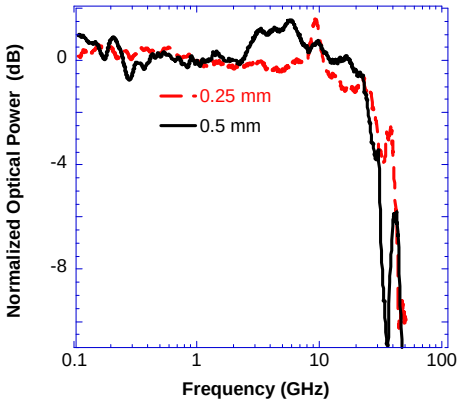

Figure 3. Measured frequency response of the modulator.

The high frequency response of the modulator was measured by using a network analyzer to drive the modulator and to measure the signal on the photodetector. In order to distinguish the bandwidth limiting effects associated with cabling from the actual bandwidth performance of the device, the RF transmission response through the cables is measured, and the net performance of the device is then obtained by subtracting the measured cable response from the total response of the modulator plus the cables. No attempt was made to impedance match the Mach Zehnder modulator to the 50-Ω impedance of the RF source. Any losses from this impedance mismatch is neither measured nor compensated for by this method.

Fig. 3 shows the small signal frequency response of the modulator after correction for frequency dependent cable losses. A 3-dB cut-off frequency of 26 GHz is reached in a 0.5 mm device, and a shorter device with 0.25 mm long phase shifters exhibits between 30-40 GHz of bandwidth. When running the 0.5 mm device in a push-pull configuration, 46 mW of RF power achieves ~33% modulation depth for a 26 GHz sinusoid. We estimate that 500 mW of power should be necessary to achieve 10 dB of extinction.

The optical loss of the device was also measured. There was 10 dB total loss from fiber to fiber (using lensed fibers for both input and output) of which approximately 5 dB is on-chip loss.

4. Conclusion

We have demonstrated a silicon modulator with two complementary outputs, a $V_\pi L$ of 2 V·cm, and a 3-dB bandwidth of 26 GHz. A modulation depth of 33% was achieved using only 40 mW of RF power. The insertion

loss of the device is 10 dB, about half of which occurs on chip, and half of which occurs coupling in and out of the device.

5. Acknowledgement

The Lincoln Laboratory portion of this work was sponsored by the EPIC Program of the Defense Advanced Research Projects Agency under Air Force Contract FA8721-05-C-0002. The work on MIT Campus was sponsored by the DARPA EPIC Program under contract W911NF-04-1-0431. Opinions, interpretations, conclusions, and recommendations are those of the authors, and do not necessarily represent the view of the United States Government.

6. References

[1] A. Liu, L. Liao, D Rubin, H. Nguyen, G. Ciftcioglu, Y. Chetrit, N. Izhaky, and M. Paniccia, "High-speed optical modulation based on carrier depletion in a silicon waveguide," Opt. Express, **15**, 660-668 (2007).

[2] K. Solehmainen, M. Kapulainen, M. Harjanne, and T. Aalto, "Adiabatic and multimode interference couplers on silicon-on-insulator," IEEE Phot. Tech. Lett. **18,** 2287-2289 (2006).

[3] J. C. Twichell, and R. Helkey, "Phase-encoded optical sampling for analog-to-digital converters," IEEE Phot. Tech. Lett. **12**, 1237-1239 (2000).

[4] F. X. Kärtner, R. Amatya, M. Araghchini, J. Birge, H. Byun, J. Chen, M. Dahlem, N. A. DiLello, F. Gan, C. W. Holzwarth, J. L. Hoyt, E. P. Ippen, A. Khilo, J. Kim, M. Kim, A. Motamedi, J. S. Orcutt, M. Park, M. Perrott, M. A. Popović, R. J. Ram, H. I. Smith, G. R. Zhou, S. J. Spector, T. M. Lyszczarz, M. W. Geis, D. M. Lennon, J. U. Yoon, M. E. Grein, and R. T. Schulein, "Photonic analog-to-digital conversion with electronic-photonic integrated circuits," in Proceedings of *SPIE Photonics West*, (Invited Paper), San Jose, CA, USA, Jan. 2008.

[5] T. Shoji, T. Tsuchizawa, T. Watanabe, K. Yamada, and H. Morita, "Spot-size converter for low-loss coupling between 0.3-μm-square Si wire waveguides and single-mode fibers", *EOS 2002. 2002 IEEE/LEOS Annual Meeting Conference Proceedings* **1**, 289-290 (2002).